Received: 14 July 2020 | Revised: 3 June 2021 | Accepted: 21 August 2021

DOI: 10.1002/mma.7808

RESEARCH ARTICLE

WILEY

Modeling the effects of information-dependent vaccination behavior on meningitis transmission

Bruno Buonomo[1] | **Alberto d'Onofrio**[2,3] | **Semu Mitiku Kassa**[4,5] | **Yetwale Hailu Workineh**[4,6]

[1]Department of Mathematics and Applications, University of Naples Federico II, Naples, Italy

[2]International Prevention Research Institute, Lyon, France

[3]37 Quai du Docteur Gailleton, Lyon, 69002, France

[4]Department of Mathematics, Addis Ababa University, Addis Ababa, Ethiopia

[5]Department of Mathematics and Statistical Sciences, Botswana International University of Science and Technology, Palapye, Botswana

[6]Department of Mathematics, Debre Markos University, Debre Markos, Ethiopia

Correspondence
Bruno Buonomo, Department of Mathematics and Applications, University of Naples Federico II, via Cintia, I-80126 Naples, Italy.
Email: buonomo@unina.it

Communicated by: M. Lachowicz

Funding information
BIUST Initiation grant, Grant/Award Number: DVC/RDI/2/1/161(34)

We propose a mathematical model to investigate the effects of information–dependent vaccination behavior on meningitis transmission. The information is represented by means of information index as early proposed by d'Onofrio et al. (Theor. Popul. Biol., 2007). We perform a qualitative analysis based on stability theory, focusing to the global stability of the disease-free equilibrium (DFE) and the related transcritical bifurcation taking place at the threshold for the DFE. Finally, we assess the role of epidemiological and information parameters in the model dynamics through numerical simulations. Our simulations suggests that the impact of the parameters that are related to human behavior critically depend on the average information delay. For example, it can induce recurrent epidemics, provided that transfer rate from the carrier to the infectious state is over a threshold. Otherwise, the endemic equilibrium is (at least) locally stable.

KEYWORDS

epidemic model, information, meningitis, vaccination

MSC CLASSIFICATION

92C60 (34D20)

1 | INTRODUCTION

Meningitis is an inflammation of the meninges, the protective membrane that surrounds the brain and spinal cord. Meningitis is mainly caused by bacteria or viruses, although it may be rarely caused also by fungi, parasites, or free-living microscopic ameba.[1] Viral meningitis is more common than bacterial meningitis but often less severe. This last can be deadly if not treated right away.[1]

Meningococcal disease (MD) is a serious bacterial form caused by *Neisseria meningitidis* bacteria, which has the potential to cause large epidemics. It can cause severe brain damage and is associated with high fatality: it is fatal in 50% of cases if untreated. This form of meningitis is observed worldwide, but the highest burden of the disease is in the

Alberto d'Onofrio is no longer a member of the IPRI as of June 15, 2020.

"meningitis belt," an area of sub-Saharan Africa that stretches from Senegal in the west to Ethiopia in the east, where around 30 000 cases are reported each year.[2]

N. meningitidis bacteria are transmitted from person-to-person through respiratory droplets or throat secretions from carriers. The transmission of *N. meningitidis* is facilitated during mass gatherings (as pilgrimages and jamborees).[2] Most cases are acquired through exposure to asymptomatic carriers and relatively few through direct contact with patients with MD.[3]

There are 12 different types of *N. meningitidis*, called serogroups, that have been identified. Only six of them (A, B, C, W, X, and Y) can cause epidemics.[2] The *N. meningitidis* serogroup A (NmA) is the most commonly isolated pathogen in the African meningitis belt,[4–6] where it has historically accounted for 90% of MD cases and the majority of large-scale epidemics.[1]

Mathematical modeling have the potential, and offer a promising way, to design effective prevention and control strategies. An early approach to modeling the spread of meningitis is due to Pinner et al[7] where the weekly *attack rate* (i.e., the number of individuals who get infected divided by the number of people at risk for the infection) was estimated for both the vaccinated and nonvaccinated populations during an epidemic of NmA in Nairobi, Kenya, in 1989.

The age structure of population has been often considered as an important modeling aspect in models of meningococcal infection spread. Martcheva and Crispino-O'Connell[8] used an age-structured meningitis model to identify the contribution of the carriers (infected who have the bacteria but appear healthy) to the transmission of MD. Tuckwell et al[9] proposed a discrete time model including age-dependent rates to determine the impact of vaccination schedule on the time course of a meningococcal serogroup C (NmC) disease in France. An age-structured model was developed by Trotter et al[10] and then fitted to data on immunization with NmC conjugate vaccines in England and Wales to investigate the effects of a conjugate vaccine program. Deterministic compartmental models were fitted to age structured data sets of MD by Coen et al.[11]

In recent years, mathematical models for MD based on the Susceptible–Carrier–Infectious–Recovered (SCIR) structure have received much attention by scholars. Simpson and Roberts[12] used an SCIR model to estimate the long-term effects of the 2004 vaccination campaign on the epidemic of meningococcal B disease in New Zealand. A SCIR model developed by Blyuss[13] and Irving et al.[14] (where they also developed some other SCIR-related models) suggested that temporary population immunity is an important factor to include in models designed to attempt to predict meningitis epidemics and to measure the efficiency of vaccines being deployed. Djatcha Yaleu et al[15] considered vaccination in an SCIR model for the dynamical transmission of NmA. They conclude that the control of the epidemic of NmA is effective if the vaccination covers a large proportion of young susceptible individuals and if the vaccine is with a high level of efficacy.

An important factor which has not been included in meningitis models, as far as we know, is the change of social behavior of individuals as a consequence of information and rumors on the spread of the disease within their community.[16,17] This phenomenon is a key factor regulating the propensity of individuals in adopting nonmandatory protective measures. Well known examples are the vaccination for childhood diseases like measles, mumps and rubella,[17] and bed-nets for mosquito-borne diseases.[18] Also in the case of meningitis, there is evidence that the perceptions of individuals about the disease affect their decisions regarding therapeutic and preventive interventions.[19] This, in turn, influences disease occurrence, morbidity, and mortality. Specific studies regarding vaccination against Meningococcal C revealed that parents' perceived vulnerability and perceived control in preventing the infection seem to influence parents' evaluation of the vaccination program. Therefore, these perceptions may, in principle, affect vaccination behavior and could be relevant to be taken into account when educating population about vaccination.[20] Another interesting investigation is the recent study focused on evaluating the knowledge and attitudes about Meningococcal B and the relative vaccine for children among a sample of parents in Italy[21] (see also a similar survey in Poland[22]). One of the conclusions, only apparently trivial, was that people who knew that the vaccine was a preventive measure of meningitis were more likely to have a positive attitude towards vaccination. On the other hand, in spite of the great successes obtained by immunization programs (as the long-term strategies in the African meningitis belt with vaccine *MenAfriVac*® against NmA meningitis[23]), vaccine hesitancy threatens to erode these gains[23,24] and push health policy makers to plan specific interventions.[25]

The feedbacks of human behavior on the transmission and control of infections is the main focus of the recently emerging research field of behavioral epidemiology (BE) of infectious diseases.[16,17] Indeed, in classical epidemic models,[26,27] individuals are modeled as passive particles randomly interacting according to the mass-action principle of statistical physics,[17] as they were reacting molecules of chemistry. This paradigm (and equivalent paradigms frequently used in individual-based models) does not account the role of human decisions in influencing the spread and the control of infectious diseases, which are instead explicitly modeled in the framework of BE (by using mean field or individual-based approaches).[28]

Vaccines for meningitis like *MenAfriVac* are given in mass for ages usually between 1 and 29.[29,30] A possible way to model behavior-dependent vaccination at all ages relies on adopting the information-based approach, which focuses on the case where the driving force of the vaccine demand is represented by the time changes in the perceived risk of infection. This approach has been introduced in d'Onofrio et al[31,32] by the means of a phenomenological model where the vaccination rates of newborn is an increasing function of the information acquired on the spread of the infectious disease. Main applications includes vaccines targeted at childhood infectious diseases such as measles, mumps, and pertussis.[16,17,31–34] Only few applications, as far as we know, are focused on the case of vaccination at all ages.[32,34-36]

In this paper, motivated by the SCIR model developed in Irving et al[14] and its variants,[12,15] we propose a mathematical model of meningitis transmission including information-dependent vaccination at all ages. The main aim is to theoretically assess, through the proposed model, how the information may affect the dynamics of meningitis transmission within a given population. We will make use of analytical methods for dynamical systems, like stability and bifurcation theory. The theoretical evaluation of the effects of human decision on the disease control will be complemented by means of numerical simulations.

The paper is organized as follows: The model is presented in Section 2. In Section 3, the basic properties of the model are given as well as the determination of the basic reproduction number. We also show that an endemic equilibrium is possible and it is unique. In Section 4, we provide a stability analysis of the disease-free equilibrium (DFE) and show, through bifurcation analysis, that the endemic equilibrium is stable, at least when the basic reproduction number is close to its critical value. In Section 5, numerical simulations are illustrated. Conclusions are given in Section 6.

2 | THE MODEL

We assume that a given population may be divided into five distinct compartments: the susceptible individuals (S), who are susceptible to be infected; the vaccinated individuals (V), who are assumed to be protected by an ideal vaccine that confer lifelong and perfect (i.e., 100%) protection; the carriers (C), who are carrying the infection and are infectious but show no signs of the invasive disease; the infectious (I), who have been infected by the disease and become immediately infectious; the recovered individuals (R). The total population is denoted by N. Therefore, at time t, it is

$$N(t) = S(t) + V(t) + C(t) + I(t) + R(t).$$

Individuals are assumed to be recruited into the population at a constant rate Λ. A mass vaccination for all susceptible individuals is given with rate ν, so that νS individuals are transferred to the vaccinated group V.

After making an effective contact with carriers or infectious, the susceptible individuals become carriers. The force of infection[27] of the disease, denoted as λ, will be described later. Carriers become infectious at a rate σ and recover at a rate δ. Infectious individuals recover at a rate ρ. The model takes into account both the natural death rate μ and disease-induced mortality rate d. Recovery from the disease is not permanent, so we assume that the recovered individuals become susceptible again at rate ϕ.

Therefore, the baseline model is governed by the following system of nonlinear ordinary differential equations:

$$\begin{aligned}
\dot{S} &= \Lambda - \lambda(N)S - \nu S + \phi R - \mu S,\\
\dot{V} &= \nu S - \mu V,\\
\dot{C} &= \lambda(N)S - (\sigma + \delta + \mu)C,\\
\dot{I} &= \sigma C - (\rho + \mu + d)I,\\
\dot{R} &= \delta C + \rho I - (\phi + \mu)R,
\end{aligned} \tag{1}$$

where the upper dots denote the time derivatives. As for the force of infection $\lambda(N)$, due to the asymptomatic nature of carriers, their contact rate is supposed to be not less than that of infectious (in line with Djatcha Yaleu et al.[15]), which are subject to identification and hospitalization. Therefore, the level of infectiousness of C is greater than or equal to I, say, by $\epsilon \geq 1$ factor.[15] The impact of this parameter on the system behavior will be discussed later. As a consequence, the force of infection is given by

$$\lambda(N) = \beta \frac{\epsilon C + I}{N}, \tag{2}$$

where $\epsilon \geq 1$ and β is the transmission rate of the infection.

Note that if $d = 0$ (and, of course, in absence of the disease), then the steady state value of the population is $\tilde{N} = \Lambda/\mu$, since the dynamics of $N(t)$ is ruled by

$$\dot{N} = \Lambda - \mu N. \tag{3}$$

Now, we will build a behavioral variant of model (1) by introducing an information-dependent vaccination. Following the approach of information-dependent models,[17,31] we assume that the vaccination rate ν is an increasing function of an information index M, which summarizes the information about the current and past values of the disease:[17,31]

$$M(t) = \int_{-\infty}^{t} g(C(\tau), I(\tau)) K_a(t-\tau) d\tau. \tag{4}$$

Here, the function g describes the role played by the infectious size in the information dynamics and is assumed to be dependent on the prevalence, that is, on the compartments C and I (the basic properties of g will be specified later). The term K_a is the delay kernel function, which represents the weight given to past prevalence. The information variable M is described by a distributed delay for two main reasons. On the one hand, people may have memory of past epidemics: indeed vaccine-related decision seldom depends on the current state of the spread of the disease. On the other hand, a delay in people awareness may be consequence of the time-consuming routine procedures (like clinical tests, notification of cases, reporting delays to public health authorities, etc.) that precede the dissemination of information on the disease's status in the community.

Combining (1) and (4), model (1) is modified in the following nonlinear integro-differential system:

$$\begin{aligned}
\dot{S} &= \Lambda - \lambda(N)S - \nu(M)S + \phi R - \mu S,\\
\dot{V} &= \nu(M)S - \mu V,\\
\dot{C} &= \lambda(N)S - (\sigma + \delta + \mu)C,\\
\dot{I} &= \sigma C - (\rho + \mu + d)I,\\
\dot{R} &= \delta C + \rho I - (\phi + \mu)R,\\
M(t) &= \int_{-\infty}^{t} g(C(\tau), I(\tau)) K_a(t-\tau) d\tau,
\end{aligned} \tag{5}$$

where $\lambda(N)$ is given in (2) and the function $\nu(M)$ models the information-dependent rate of vaccinations, and it may be split as follows:

$$\nu(M) = \nu_0 + \nu_1(M), \tag{6}$$

where ν_0 is a positive constant representing the fraction of susceptibles that are vaccinated independently on the available current and historical information on the prevalence level of the disease and $\nu_1(M)$ models the fraction of susceptibles that are vaccinated depending on the social alarm caused by the disease.[31]

The following basic assumptions are made regarding the functions $g(C, I)$ and $\nu_1(M)$: (i) $g(C, I)$ and ν_1 are continuous and differentiable, except in some cases, at finite number of points; (ii) $g(0, 0) = 0$, and $\nu_1(0) = 0$; (iii) $g(C, I)$ and ν_1 are positive for any positive value of their respective arguments; (iv) $0 < \partial g/\partial C < c_1$, $0 < \partial g/\partial I < c_2$, and $0 < \nu 1'(M) < c_3$, for some constants c_1, c_2, and c_3.

The simplest specific functional form of $\nu_1(M)$ is the linear function,

$$\nu_1(M) = bM, \tag{7}$$

where b is a positive constant. Moreover, since the possibility of getting information about carriers group C is almost not possible, we take g as a function of only the infected groups I. Again, the simplest form is

$$g(I) = h\frac{I}{\tilde{N}} = kI. \tag{8}$$

Note that the size of the infectious compartment is normalized by dividing I by the reference steady state population. In this case, the positive constant parameter h can be interpreted as the *information coverage*. This may be seen as a "summary" of two contrasting phenomena: the phenomenon of disease underreporting and the level of media and rumors coverage of the status of the disease, which tends to amplify the social alarm.[33]

TABLE 1 Description and baseline values of the parameters of model (10)

Parameter	Description	Value (range)	Unit	Source and comments
μ	Per-capita natural mortality rate for all classes	0.02	years^{-1}	Life expectancy is 50 years[14]
$\tilde{N}$	Steady state Population	1000000	adim.	Assumed
Λ	Inflow rate of susceptible individuals	20000	years^{-1}	$= \mu\tilde{N}$
β	Transmission Rate	100 (50, 200)	years^{-1}	Irving et al.[14]
ρ	Rate of recovery of infectious individuals	52	years^{-1}	Disease duration $\approx$1 week[14]
d	Disease-induced death rate	5.2	years^{-1}	Mortality probability $\approx$0.1[14]
σ	Rate moving from carrier to infected	26 (0.1,52)	years^{-1}	Irving et al.[14]
δ	Recovery rate of carriers	26 (0.1, 52)	years^{-1}	Irving et al.[14]
ϕ	Rate of loss of immunity	0.1 (0.04, 2)	years^{-1}	Irving et al.[14]
ν_0	Behavior-independent vaccination rate	0.04	years^{-1}	Assumed
T	Average information delay	[0, 120]	days	From no delay to 4 months about.
a	Inverse of average information delay	$365.25/T$	years^{-1}	Inverse of T in years^{-1}
b	Slope of vaccination rate w.r.t. information index M	2000 $(1, \infty)$	years^{-1}	Assumed
h	Information coverage	0.5 (0.1, 1)	adim.	Assumed
ϵ	Enhanced infectiousness of carriers	1.3	adim.	Assumed

As far as the kernel $K_a(t)$ is concerned, a relevant example is the weak exponential delay kernel[37]

$$K_a(t) = a\, e^{-at}, \tag{9}$$

where the parameter a assumes the biological meaning of inverse of the average delay of the collected information on the disease, as well as the average length of the historical memory concerning the disease in study. The kernel (9) is a particular case of Erlangian distribution. This choice has the advantage of making the corresponding integro-differential system reducible into ordinary differential equations through the *linear chain trick*.[37] Model (5)–(2)–(4), with choices (6), (7), (8), and (9), may be written

$$\begin{aligned}
\dot{S} &= \Lambda - \lambda(N)S - (\nu_0 + bM)S + \phi R - \mu S,\\
\dot{V} &= (\nu_0 + bM)S - \mu V,\\
\dot{C} &= \lambda(N)S - (\sigma + \delta + \mu)C,\\
\dot{I} &= \sigma C - (\rho + \mu + d)I,\\
\dot{R} &= \delta C + \rho I - (\phi + \mu)R,\\
\dot{M} &= a\,(kI - M)
\end{aligned} \tag{10}$$

and will be the subject of the investigation in this paper. The parameters, their descriptions, and the baseline values are given in Table 1.

3 | BASIC PROPERTIES

We begin by determining the biologically feasible set for model (10). The following proposition also implies that the solutions of (10) are bounded, provided that the initial conditions are nonnegative.

Proposition 1. *The set*

$$\Omega = \left\{ (S, V, C, I, R, M) \in \mathbf{R}^6_+ \,:\, 0 \le M \le k\tilde{N},\;\; 0 \le \tilde{N}\frac{\mu}{\mu + d} \le S + V + C + I + R \le \tilde{N} \right\} \tag{11}$$

is positively invariant and absorbing.

Proof. It suffices to note that adding the first five equations of (10), it follows

$$\dot{N} = \Lambda - \mu N - dI, \tag{12}$$

so that from

$$\Lambda - (\mu + d)N \le \dot{N} \le \Lambda - \mu N,$$

it follows

$$\limsup_{t\to\infty} N(t) \le \tilde{N},$$
$$\liminf_{t\to\infty} N(t) \le \frac{\Lambda}{\mu+d} = \tilde{N}\frac{\mu}{\mu+d}.$$

Then, the rest of the proof follows from standard arguments as in Buonomo et al.[33] □

It is easy to check that model (10) admits the DFE, which represents the scenario where there is no infection within the community, given by

$$E_0 = (S_0, V_0, 0, 0, 0, 0), \tag{13}$$

where

$$S_0 = \frac{\Lambda}{\mu+\nu_0}; \quad V_0 = \frac{\nu_0\Lambda}{\mu(\mu+\nu_0)}.$$

Our next step is to determine the basic reproduction number (BRN) $\mathcal{R}_0$ associated to model (10). To this aim, we apply the *next generation matrix method* (NGM).[38] According to the well-known procedure,[38] we identify (C, I) and (S, V, R) as the infected and uninfected classes, respectively. Then, we can write the matrix $\mathcal{F}$ for the new infection and the matrix $\mathcal{V}$ for the remaining transfer. More precisely, the matrix $\mathcal{F}$, where the entries represent the rates of new infections (i.e., the rate of appearance of new infections in compartments C and I), here is a column vector, actually, given by

$$\mathcal{F} = \begin{bmatrix} \lambda S \\ 0 \end{bmatrix} = \begin{bmatrix} \frac{\beta}{N}(\epsilon C + I)S \\ 0 \end{bmatrix}.$$

The matrix $\mathcal{V}$ where the entries represent the rate of infections transferred (i.e., it incorporates the remaining transitional terms, namely, births, deaths, disease progression, and recovery in C and I), is also a vector, here, given by:

$$\mathcal{V} = \begin{bmatrix} (\sigma+\delta+\mu)C \\ -\sigma C + (\rho+\mu+d)I \end{bmatrix}.$$

According to NGM, the BRN $\mathcal{R}_0$ is the greatest of the eigenvalues of the matrix FV^{-1}, where F and V are the matrices obtained by differentiating $\mathcal{F}$ and $\mathcal{V}$ with respect to C and I and then evaluated at the DFE E_0. In our case, we have

$$\tilde{F} = \begin{bmatrix} \frac{\beta S(\epsilon N - \epsilon C - I)}{N^2} & \frac{\beta S(N - \epsilon C - I)}{N^2} \\ 0 & 0 \end{bmatrix}, \quad \tilde{V} = \begin{bmatrix} (\sigma+\delta+\mu) & 0 \\ -\sigma & (\rho+\mu+d) \end{bmatrix},$$

and therefore,

$$F = \tilde{F}(E_0) = \begin{bmatrix} \frac{\beta\epsilon\mu}{\mu+\nu_0} & \frac{\beta\mu}{\mu+\nu_0} \\ 0 & 0 \end{bmatrix}, \quad V = \tilde{V}(E_0) = \begin{bmatrix} (\sigma+\delta+\mu) & 0 \\ -\sigma & (\rho+\mu+d) \end{bmatrix}.$$

It can be easily checked that

$$FV^{-1} = \begin{bmatrix} \frac{\beta\epsilon\mu}{(\mu+\nu_0)(\sigma+\delta+\mu)} + \frac{\beta\mu\sigma}{(\mu+\nu_0)(\sigma+\delta+\mu)(\rho+\mu+d)} & \frac{\beta\mu}{(\rho+\mu+d)} \\ 0 & 0 \end{bmatrix},$$

and hence the BRN is given by

$$\mathcal{R}_0 = \frac{\beta\epsilon\mu}{(\mu+\nu_0)(\sigma+\delta+\mu)} + \frac{\beta\mu\sigma}{(\mu+\nu_0)(\sigma+\delta+\mu)(\rho+\mu+d)}. \tag{14}$$

The existence and uniqueness of an endemic equilibrium, which represent a steady state prevalence of the disease in the population, is given in the following proposition:

Proposition 2. *Model (10) admits a unique endemic equilibrium for* $\mathcal{R}_0 > 1$.

Proof. Let us denote the generic equilibrium (i.e., the vector solution with positive constant components) as $E^* = (S^*, V^*, C^*, I^*, R^*, M^*)$. From (10), it follows:

$$S^* = \frac{(\sigma+\delta+\mu)(\rho+\mu+d)}{\sigma\lambda^*}I^*, \quad V^* = \frac{(\nu_0+bM^*)S^*}{\mu} = \frac{(\nu_0+bkI^*)(\sigma+\delta+\mu)(\rho+\mu+d)}{\mu\sigma\lambda^*}I^*,$$
$$C^* = \frac{(\rho+\mu+d)}{\sigma}I^*, \quad R^* = \frac{\delta(\rho+\mu+d)+\sigma\rho}{\sigma(\phi+\mu)}I^*, \quad M^* = kI^*.$$

where

$$\lambda^* = \beta\frac{\epsilon C^* + I^*}{N^*},$$

and I^* is the positive solution of

$$b_2 I^{*2} + b_1 I^* + b_0 = 0, \tag{15}$$

where

$$b_2 = \sigma bkd\, b_3,$$

$$b_1 = \sigma d(\nu_0+\mu)b_3 - \Lambda\sigma bk\, b_3 + \beta\mu\phi\left[\delta(\rho+\mu+d)+\sigma\rho\right]\left[\epsilon(\rho+\mu+d)+\sigma\right] - b_3\beta\mu\left[\epsilon(\rho+\mu+d)+\sigma\right],$$

$$b_0 = \sigma\Lambda(\nu_0+\mu)b_3[\mathcal{R}_0 - 1],$$

and

$$b_3 = (\phi+\mu)(\sigma+\delta+\mu)(\rho+\mu+d).$$

Let

$$f(I^*) = b_2 I^{*2} + b_1 I^* + b_0. \tag{16}$$

Note that $f'(I^*) = b_2 > 0$, and $f(0) = b_0 > 0$ for $\mathcal{R}_0 > 1$. Moreover, since $N^* > 0$, from (12), it follows $I^* < \frac{\Lambda}{d}$, and direct calculations reveal that

$$f\left(\frac{\Lambda}{d}\right) = -\beta\mu\frac{\Lambda}{d}\left[\epsilon(\rho+\mu+d)\sigma\right]\left\{\mu\delta\rho + \mu\sigma\rho + (\phi+\mu)\mu\left[(\rho+\mu+d)+\sigma\right] + \delta\mu^2 + \mu\delta d\right\} < 0.$$

Therefore, the function f has only one zero on $\left[0, \frac{\Lambda}{d}\right]$, implying that the endemic equilibrium is unique provided that $\mathcal{R}_0 > 1$, whereas and no endemic equilibria are admissible for $\mathcal{R}_0 < 1$. □

4 | STABILITY OF EQUILIBRIA

We begin with the following local stability result:

Proposition 3. *If $\mathcal{R}_0 < 1$, then E_0 is locally asymptotically stable in Ω, and unstable if $\mathcal{R}_0 > 1$.*

Proof. This result is a direct consequence of the NGM used in Section 3; see Theorem 2 in van den Driessche and Watmough.[38] □

In epidemiological terms, Proposition 3 states that it is possible to control the epidemic if we can reduce the value of $\mathcal{R}_0 < 1$ as long as the initial population is in the neighborhood of the DFE point E_0. However, it is not difficult to show that for $\mathcal{R}_0 < 1$ the elimination of the disease happens independently from the initial size of the population. In other words, E_0 is globally asymptotically stable (GAS) for $\mathcal{R}_0 < 1$. This is stated in the following Proposition.

Proposition 4. *If $\mathcal{R}_0 < 1$, then E_0 is globally asymptotically stable in Ω.*

Proof. This result can be obtained by checking that all the (five) hypotheses of Theorem 4.3 in Kamgang and Sallet[39] are satisfied. This procedure is well known and used elsewhere (see, e.g., Theorem 2 in the recent paper[40]). For our model, the result can be obtained in the same way. Therefore, for the sake of brevity, we omit the details. □

Remark 1. We note that $\mathcal{R}_0$ given in (14) does not depend on behavior-related parameters. The condition $\mathcal{R}_0 > 1$ in Proposition 4 may be realized, through vaccination, only if the baseline vaccination rate ν_0 is sufficiently large. However, it is unlikely that this can actually be done in practice. In other words, the result in Proposition 4 essentially means that the elimination of the disease is impossible under nonmandatory vaccination that is driven by information.

As far as the stability of the endemic equilibrium E^* is concerned, it is difficult to obtain an analytical stability result, even through the linearization method. However, we can use a bifurcation theory approach to get an insight on the stability properties of the model (and therefore of E^*) for values of the BRN close to the critical value $\mathcal{R}_0 = 1$. We know that the DFE E_0 is a *nonhyperbolic* equilibrium for $\mathcal{R}_0 = 1$ (this follows because the Jacobian matrix of system (10), evaluated at E_0, admits a zero eigenvalue) and we also know from Proposition 2 that there is an endemic equilibrium branch bifurcating from E_0 at $\mathcal{R}_0 = 1$. What we are interested in is to check that such a branch is stable, at least when BRN is close to the critical value $\mathcal{R}_0 = 1$ (in such case, the bifurcation is a *transcritical forward bifurcation*[41]). To this aim, we study the center manifold at the *criticality* (i.e., at E_0 for $\mathcal{R}_0 = 1$) by using the approach developed in previous works,[38,41,42] which establishes that the normal form representing the dynamics of the system on the center manifold is given by

$$\dot{y} = A_1 \phi y + A_2 y^2,$$

where ϕ denotes a bifurcation parameter to be chosen, and

$$A_1 = v \cdot D_{x\phi} f(x_0, 0) u \equiv \sum_{k,i,j=1}^{n} v_k u_i \frac{\partial^2 f_k(x_0,0)}{\partial x_i \partial \phi}. \tag{17}$$

and

$$A_2 = \tfrac{v}{2} \cdot D_{xx} f(x_0, 0) u^2 \equiv \tfrac{1}{2} \sum_{k,i,j=1}^{n} v_k u_i u_j \frac{\partial^2 f_k(x_0,0)}{\partial x_i \partial x_j}, \tag{18}$$

where f_k, $k = 1, \dots, n$ denote the right hand sides of the system (10), x denotes the state vector, x_0 the DFE E_0 and v and u denote the left and right eigenvectors, respectively, corresponding to the zero eigenvalue of the Jacobian matrix of system (10) evaluated at the criticality.

In our case, let us choose β as bifurcation parameter. Observe that $\mathcal{R}_0 = 1$ is equivalent to

$$\beta = \beta^* := \frac{(\mu + \nu_0)(\sigma + \delta + \mu)(\rho + \mu + d)}{\mu \left[\epsilon(\rho + \mu + d) + \sigma\right]}, \tag{19}$$

so that the DFE E_0 is (globally) stable when $\beta < \beta^*$ and is unstable when $\beta > \beta^*$. Therefore, β^* is a bifurcation value.

The direction of the bifurcation occurring at $\beta = \beta^*$ can be derived from the sign of coefficients (18) and (17). More precisely, if $A_1 > 0$ and $A_2 < 0$, then at $\beta_1 = \beta^*$ there is a forward bifurcation.[41]

In our case, we have the following:

Theorem 1. *System (10) exhibits a forward bifurcation at E_0 and $\mathcal{R}_0 = 1$.*

Proof. The Jacobian matrix of system (10) evaluated at E_0 and $\beta = \beta^*$ is given by

$$J_{\beta^*} = \begin{bmatrix} -(\nu_0 + \mu) & 0 & -\frac{\beta^* \epsilon \mu}{\nu_0 + \mu} & -\frac{\beta^* \mu}{\nu_0 + \mu} & \phi & -\frac{b\Lambda}{\mu + \nu_0} \\ \nu_0 & -\mu & 0 & 0 & 0 & \frac{b\Lambda}{\mu + \nu_0} \\ 0 & 0 & \frac{\beta^* \epsilon \mu}{\nu_0 + \mu} - (\sigma + \delta + \mu) & \frac{\beta^* \mu}{\nu_0 + \mu} & 0 & 0 \\ 0 & 0 & \sigma & -(\rho + \mu + d) & 0 & 0 \\ 0 & 0 & \delta & \rho & -(\phi + \mu) & 0 \\ 0 & 0 & 0 & ak & 0 & -a \end{bmatrix}. \tag{20}$$

The eigenvalues are $\lambda_1 = -(\nu + \mu)$, $\lambda_2 = -\mu$, $\lambda_3 = -(\phi + \mu)$, $\lambda_4 = -a$, and two roots of the quadratic equation:

$$\varphi^2 + \left[\frac{\beta^* \epsilon \mu}{\nu_0 + \mu} - (\sigma + \delta + \mu) - (\rho + \mu + d)\right] \varphi - \frac{\beta^* \mu}{\nu_0 + \mu}(\epsilon(\rho + \mu + d) + \sigma) + (\sigma + \delta + \mu)(\rho + \mu + d) = 0.$$

From (19), it follows that

$$\varphi^2 + \left\{ \frac{(\sigma+\delta+\mu)(\rho+\mu+d)\epsilon}{\epsilon(\rho+\mu+d)+\sigma} - \left[(\sigma+\delta+\mu)+(\rho+\mu+d)\right] \right\} \varphi = 0.$$

Therefore, the remaining two eigenvalues are $\lambda_5 = 0$, and

$$\lambda_6 = -\frac{(\sigma+\delta+\mu)\sigma + (\rho+\mu+d)(\epsilon(\rho+\mu+d)+\sigma)}{\epsilon(\rho+\mu+d)+\sigma} < 0.$$

Hence, the matrix J_{β^*} has zero as a simple eigenvalue and all the other eigenvalues are real and negative.

Now, we determine the right and left eigenvectors of J_{β^*} corresponding to the zero eigenvalue. Let $u = (u_1, u_2, u_3, u_4, u_5, u_6)^T$ denote a right eigenvector associated with the zero eigenvalue $\lambda_5 = 0$, that is,

$$J_{\beta^*} u = 0.$$

After some algebraic manipulations, we get:

$$\begin{aligned}
u_1 &= \frac{\beta^*}{(\nu_0+\mu)^2}\left[-\frac{\epsilon\mu(\rho+\mu+d)}{\sigma} - \mu + \frac{\phi(\nu_0+\mu)[\delta(\rho+\mu+d)+\sigma\rho]}{\beta^*\sigma(\phi+\mu)} - \frac{bk\Lambda}{\beta^*}\right] u_4,\\
u_2 &= [\frac{\nu_0}{\mu}\frac{\beta^*}{(\nu_0+\mu)^2}\left[-\frac{\epsilon\mu(\rho+\mu+d)}{\sigma} - \mu + \frac{\phi(\nu_0+\mu)[\delta(\rho+\mu+d)+\sigma\rho]}{\beta^*\sigma(\phi+\mu)} - \frac{bk\Lambda}{\beta^*}\right] + \frac{bk\Lambda}{\mu(\mu+\nu_0)}]u_4,\\
u_3 &= \frac{(\rho+\mu+d)}{\sigma}u_4,\\
u_4 &= u_4 \geq 0,\\
u_5 &= \frac{\delta(\rho+\mu+d)+\sigma\rho}{\sigma(\phi+\mu)}u_4,\\
u_6 &= ku_4.
\end{aligned}$$

Similarly, the left eigenvectors can be determined from equation $vJ_{\beta^*} = \lambda v$, or equivalently $J_{\beta^*}^T v^T = 0$, and we get

$$v_1 = v_2 = v_5 = v_6 = 0, \quad v_3 = \frac{(\rho+\mu+d)}{\sigma}v_4, \quad v_4 = v_4 \geq 0.$$

The coefficients (18) and (17) can now be computed. It follows that

$$A_1 = v_3\left[\frac{\mu}{\nu_0+\mu}(\epsilon u_3 + u_4)\right],$$

and

$$A_2 = -v_3\frac{\beta^*\mu}{\Lambda(\nu_0+\mu)}\left[\frac{b\Lambda}{\mu(\nu_0+\mu)}ku_4\,(u_3\epsilon\mu + ku_4)\,u_4\mu + 2u_3^2\epsilon\mu + u_3u_4(\epsilon+1)\mu + u_3u_5\epsilon\mu + 2u_4^2\mu + u_4u_5\mu\right].$$

Therefore, we have $A_1 > 0$ and $A_2 < 0$ and the system undergoes a forward bifurcation. In other words, when $\mathcal{R}_0$ crosses the threshold value $\mathcal{R}_0 = 1$ from left to right, the DFE changes its stability from asymptotically stable to unstable and a positive endemic equilibrium E^* appears and this last is locally asymptotically stable, at least for values of $\mathcal{R}_0$ close to 1. □

Remark 2. Note that the basic reproduction number can be rewritten as follows:

$$\mathcal{R}_0 = q_1\epsilon + q_0; \tag{21}$$

thus, if

$$\epsilon \geq \epsilon^* = \frac{\max(0, 1 - q_0)}{q_1}, \tag{22}$$

then $\mathcal{R}_0 > 1$. It follows that if $q_0 < 1$, there exists a nonzero minimal threshold for ϵ that guarantees the endemicity of the disease. Moreover, if $1 - q_0 > q_1$, the threshold ϵ^* is bigger than one. With reference to Table 1, if $\beta = 100$, then $\epsilon^* = 1.114 > 1$. If instead $\beta = 150$, then $\epsilon^* = 0.569 < 1$.

5 | NUMERICAL INVESTIGATIONS

In this section, we will assess how the endemic equilibrium and the dynamics of the model depend on some key behavioral and epidemiological parameters.

In Figure 1, we consider how the steady-state number of infectious at the endemic equilibrium, I^*, depends on the normalized information coverage h (whose range is $(0, 1)$) for the following values of the sensitivity slope: $b = 1000$ (black solid line), and $b = 2000$ (red dashed line). Not surprisingly, I^* is decreasing with increasing both h and b.

As far as the simulations of the spread and control of the disease are concerned, we will consider the following initial conditions:

(i) before the introduction of the disease the population was at its steady state, thus $N(0^-) = \tilde{N}$;
(ii) one single infectious subject enters into the population: $I(0) = 1$;
(iii) No carriers and removed subjects are present at $t = 0$: $C(0) = 0$ and $R(0) = 0$;
(iv) a relatively small fraction of the population has been vaccinated: $V(0) = 0.1\tilde{N}$. It follows that $S(0) = 0.9\tilde{N} - 1$.

We first consider the epidemic scenario, by simulating the system from the initial time to one year later ($t \in [0, 1]$) as illustrated in Figures 2 and 3. Namely, in the left panel of Figure 2, we show the time-course of both C and I in the case where there is no behavioral dependence of the vaccination rate, that is, $b = 0$, which implies that $\nu(M) = \nu_0$. In both the central and right panels of Figure 2, where we set $b = 2000$, we show the cases corresponding to $T = 10$ days and

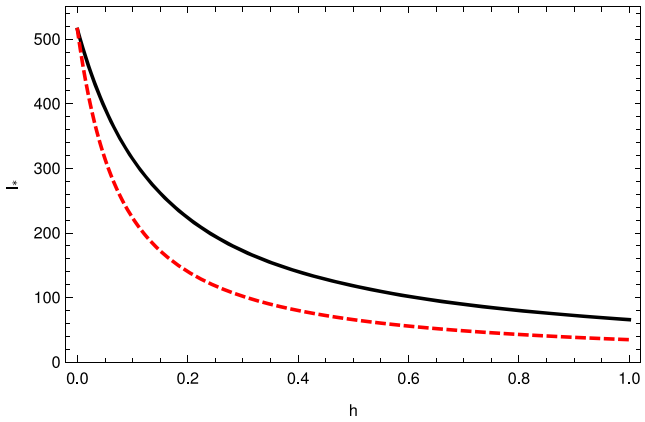

FIGURE 1 Endemic equilibrium for I vs. normalized information coverage h. Solid black line: $b = 1000$, dashed red line: $b = 2000$. Other parameters: as in Table 1 [Colour figure can be viewed at wileyonlinelibrary.com]

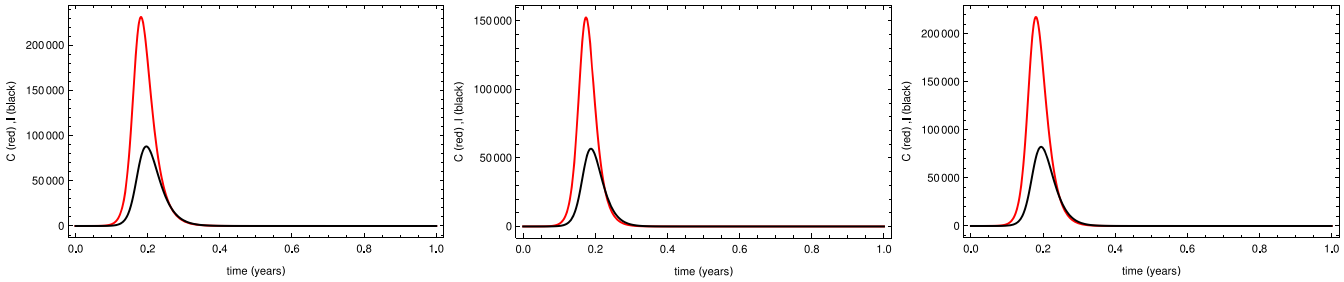

FIGURE 2 Impact of behavioral terms on the epidemics outbreak during the first year. Time courses of $C(t)$ (red) and of $I(t)$ (black). Left panel: absence of behavioral components in the vaccination ($b = 0$); central and left panel: presence of behavioral components in the vaccination ($b = 1000$). Central panel: $T = 10$ days; right panel: $T = 120$ days. In all panels, $\sigma = 26$. Other parameters as in Table 1 [Colour figure can be viewed at wileyonlinelibrary.com]

$T = 120$ days, respectively. For $T = 10$, we can see that the prompt response induces a remarkable decrease of the epidemic peak, which is no more observed for $T = 120$ days. The time course of the total population $N(t)$ during the first year is shown in Figure 3.

An analytical assessment of the onset of bifurcations is hard to obtain. Thus, given the parameter a, we computed the eigenvalues $\lambda_i(a)$. The maximum value of the real part of the $\lambda_i(1/T)$ is then plotted in Figure 4 (left panel). As it can be seen, there is an interval $T \in (T_{min}, T_{max})$ where the endemic equilibrium is unstable and steady state oscillations (not necessarily periodic) can take place. In other words, the model predict the onset of recurrent epidemics. In Figure 5, we

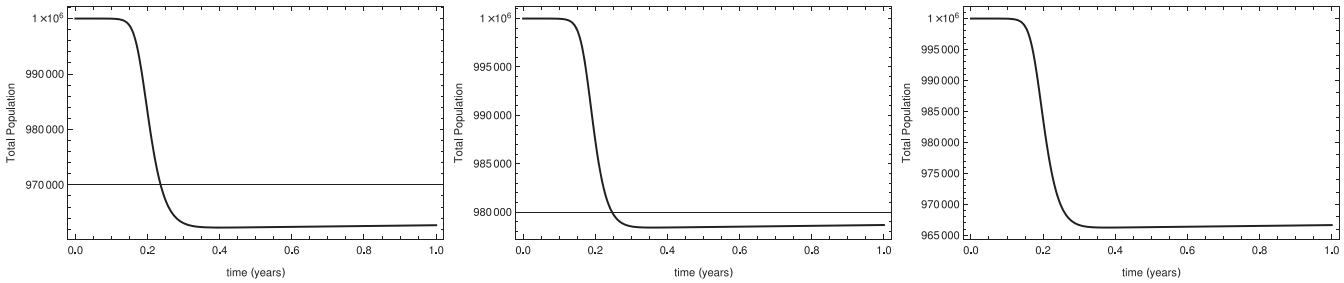

FIGURE 3 Impact of behavioral terms on the total population $N(t)$ during the epidemics outbreak. Left panel: absence of behavioral components in the vaccination ($b = 0$); central and left panel: presence of behavioral components in the vaccination ($b = 1000$). Central panel: $T = 10$ days; right panel: $T = 120$ days. In all panels, $\sigma = 26$. Other parameters as in Table 1

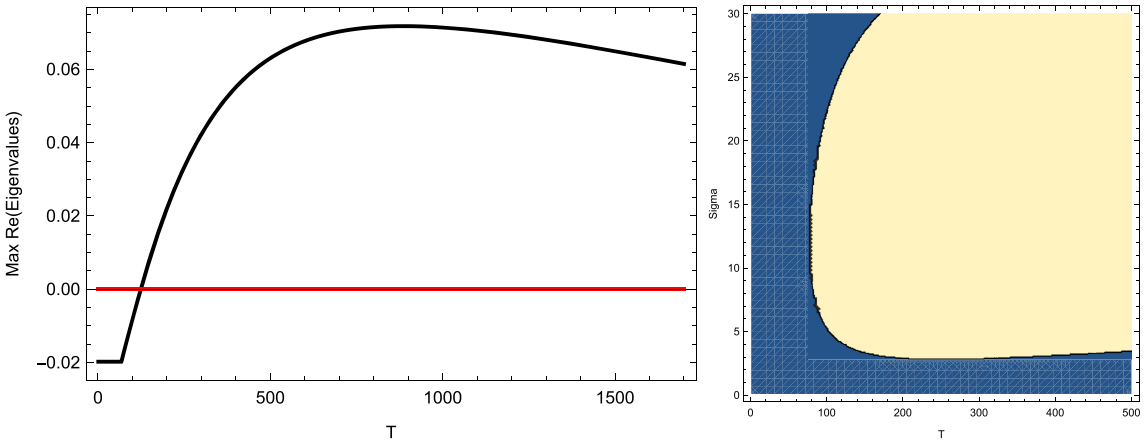

FIGURE 4 Bifurcation diagrams at the endemic equilibrium. Left panel: one bifurcation parameter, T, and $\sigma = 26$. Right panel: two bifurcation parameters: (T, σ). Other parameters as indicated in Table 1. The region of instability is in light color, and the local stability region is dark [Colour figure can be viewed at wileyonlinelibrary.com]

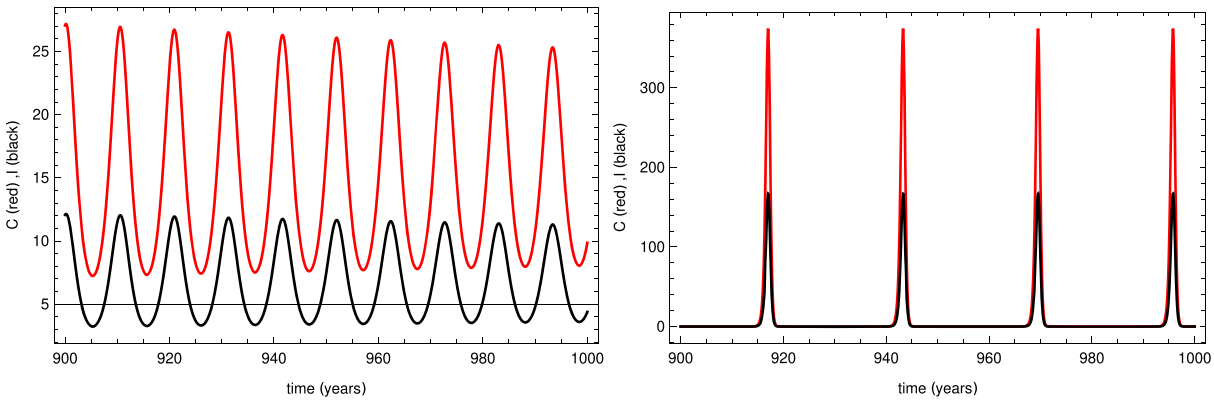

FIGURE 5 Steady state oscillations. Left panel: $T = 120$ days; right panel: $T = 220$ days. Red lines: $C(t)$, black lines: $I(t)$. Other parameters as in Table 1 [Colour figure can be viewed at wileyonlinelibrary.com]

plotted the corresponding steady-state oscillations for, respectively, $T = 120$ days (left panel), which is very close to the unstablity curve, and for $T = 220$ days (right panel). As one can see, the model predicts recurrent epidemics. Observe that for $T = 220$ days, the epidemics have larger peak and period than for $T = 120$ days.

All the above simulations were performed by assuming $\delta \approx \sigma$ (see Table 1); that is, the recovery rate of carriers is equal to the rate of moving from carriers to infected, which seems reasonable. This however causes a large infectious peak, as in the models considered by Irving et al,[14] where—however—vaccination was not considered. The presence of vaccination and of behavior-dependent increase of the vaccination rate, of course, partially mitigate this phenomenon. Irving et al[14] noticed that in their model, lower peaks of $I(t)$ are obtained by assuming $\delta >> \sigma$. Since $P_R = \delta/(\delta + \sigma)$ is the probability that an individual going out of the C compartment enters in the R compartment, the above-mentioned hypotheses is equivalent to assume that $p_R \approx 1$, that is, that the vast majority of carriers do not become infectious. To compare, the

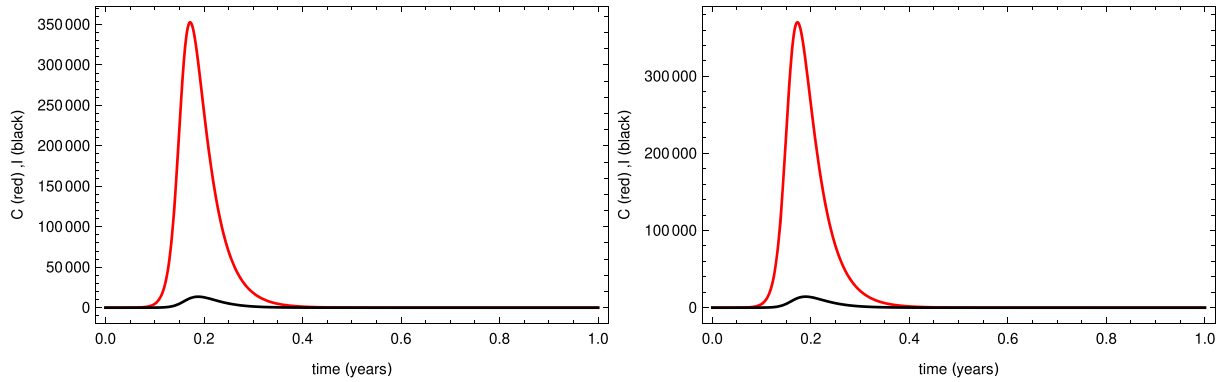

FIGURE 6 Simulations of the first year of the spread of the disease, with $\sigma = 2.6$ years^{-1}. Left panel: $T = 10$ days, right panel: $T = 120$ days. Other parameters as in Table 1 [Colour figure can be viewed at wileyonlinelibrary.com]

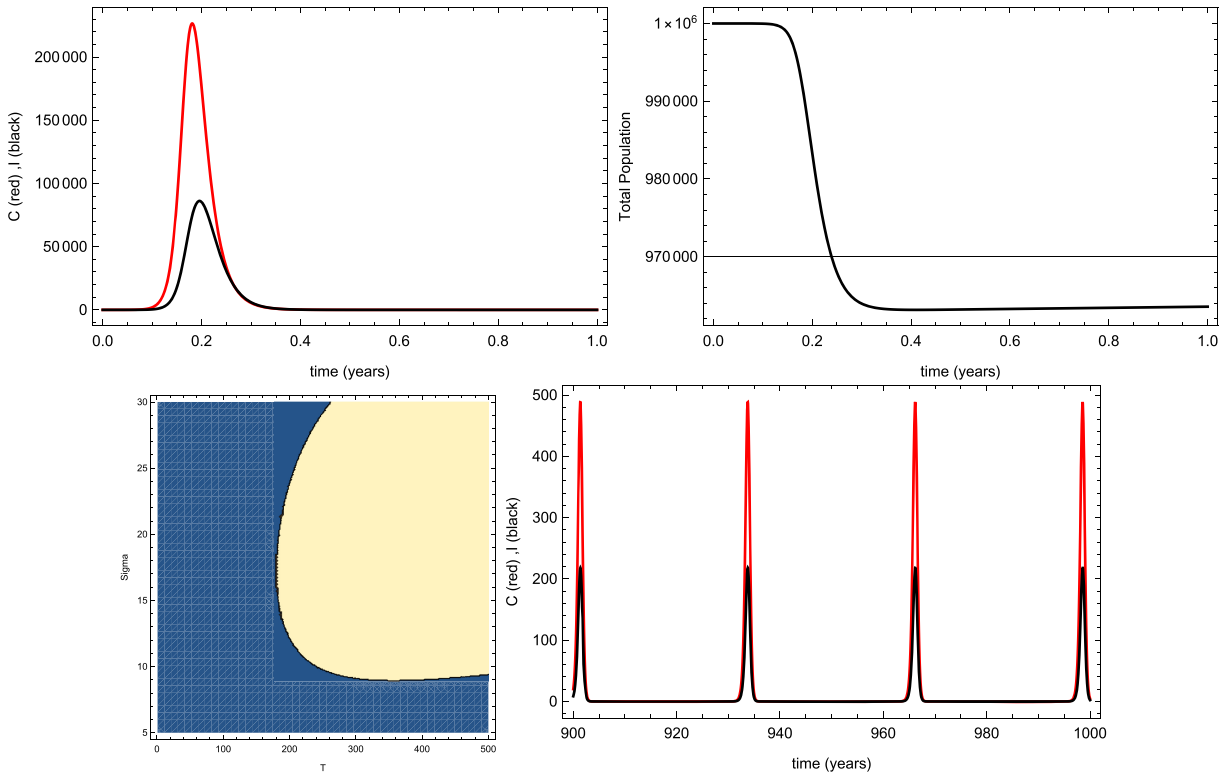

FIGURE 7 Impact of $\phi = 1.0$. Upper left panel: the time course of C and I in the first year of the epidemics; upper right panel: the time course of the population in the first year. Lower left panel: LAS region; lower right panel: steady state time courses of C and I. Here, $T_{del} = 300$ and all parameters (except ϕ) are as in Table 1 [Colour figure can be viewed at wileyonlinelibrary.com]

assumption $\delta = \sigma$ corresponds to $p_R = 0.5$, that is, that half of carriers become infectious (apart those dying for natural causes, of course).

Based on the above considerations, we computed a two-parameters bifurcation diagram (BBD) where not only T but also σ is considered as bifurcation parameter. The BBD is shown in Figure 4 (right panel), where the region of instability is in light color, and the local stability region is dark. Our numerical computations showed that (i) under a threshold value $\sigma = \sigma_m \approx 4.9$, the system is LAS, and (ii) for $\sigma \in (\sigma_m, 26)$, the endemic equilibrium is unstable in a window of values of T: $T \in (T_{min}(\sigma), T_{max}(\sigma))$ whose size $A = T_{max}(\sigma) - T_{min}(\sigma)$ increases with σ.

To show the impact of σ in the first phase of epidemics, we performed alternative simulations by setting a lower value of p_R compared to $p_R = 0.5$. Namely, we set $\delta = 10\sigma$, which implies that $p_R = 1/9$. The simulation is reported in Figure 6, where one can observe that the epidemic peak is reduced when compared to the case shown in Figure 2.

In Figure 7, where we set $\phi = 1.0$ and $T_{del} = 300$, we show that the impact of the parameter ϕ is quantitative but the qualitative behavior of the system is unchanged w.r.t. the above simulations, where $\phi = 0.1$.

In order to numerically investigate the role of ϵ, we have to consider a larger value of β w.r.t. the previous simulations since $\epsilon^*|_{\beta=100} \approx 1.114$. Thus, in Figure 8, we set $\beta = 150$. The instability regions (upper panels of Figure 8) have a remarkable change. Namely, (i) for $\epsilon = 0.8$, the instability can onset for lower values of σ w.r.t. the case $\epsilon = 1.3$; (ii) for $\epsilon = 1.3$, the instability can onset for lower values of T w.r.t. the case $\epsilon = 0.8$. The steady state oscillations for the case $\epsilon = 0.8$ have a lower peak (as expected) and a much larger period w.r.t. the case $\epsilon = 1.3$.

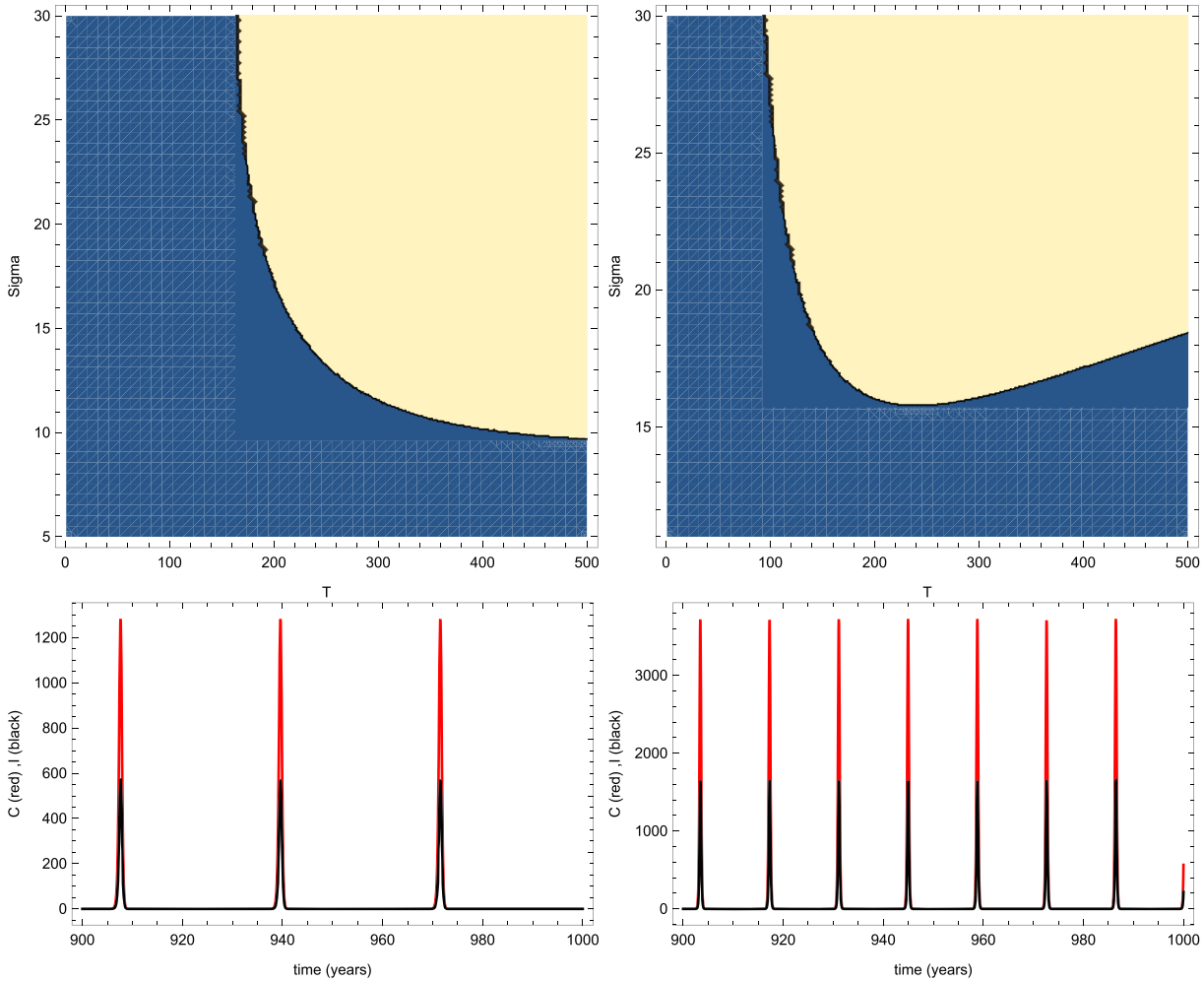

FIGURE 8 Impact of ϵ. Upper left panel: LAS region for $\epsilon = 0.8$; upper right panel: LAS region for $\epsilon = 1.3$. Lower left panel: steady state time courses of C and I for $\epsilon = 0.8$. Lower right panel: steady state time courses of C and I for $\epsilon = 1.3$. Here, $\beta = 150$, $T_{del} = 300$, $\phi = 1.0$, and all other parameters are as in Table 1 [Colour figure can be viewed at wileyonlinelibrary.com]

Finally, again concerning the impact of ϵ on the system dynamics, note that if at time t_M the prevalence has a maximum, then such a value is smaller than the value $C(t_M)$ (which is, in general, not a maximum for C) independently from the value assumed by ϵ, provided that

$$\sigma < \rho + \mu + \delta,$$

condition that is satisfied in the parametric set we considered. Indeed, since at $t = t_M$ it is $\dot{I}(t_M) = 0$, one gets from the ODE describing the dynamics of I that

$$I(t_M) = C(t_M)\frac{\sigma}{\rho + \mu + \delta} \approx \frac{1}{3}C(t_M).$$

6 | CONCLUSIONS

As far as we know, the effects of information-dependent behavior on meningitis transmission has not been studied before in the context of behavioral epidemiology.[16] Here, we propose a variant of a well established meningitis model, where an information-dependent vaccination behavior is explicitly taken into account. This is done by considering the information index as early proposed in d'Onofrio et al.[31]

The qualitative analysis of the resulting behavioral model is based on stability and bifurcation theory. These results extend (in some way) the ones obtained in previous works,[13–15] in that (i) we included behavioral effects and (ii) we get a rigorous results concerning the transcritical bifurcation taking place at the threshold $\mathcal{R}_0 = 1$.

The BRN of the model does not depend on the information-related parameters; thus, the GAS result concerning the DFE can be read (similarly to the case of the SIR model with behavioral vaccination investigated in d'Onofrio et al.[31]) as an *eradication impossible* result:[16,17] the disease elimination from the target population cannot be reached under nonmandatory vaccination that is driven by information. Indeed, to guarantee the disease eradication the baseline behavior-independent vaccination rate ought to be as great as to guarantee the eradication in absence of the behavioral effects in the vaccination rate. This is, of course, unlikely.[16,17]

Interestingly, the BRN depends on the parameter ϵ in a linear affine way, so that (depending on the values of the other parameters) there can exist a minimal threshold for ϵ such that under this threshold the disease cannot remain endemic. Moreover, this threshold can be larger than one (as it happens with the parametric set we used in this work).

As far as the effect of information is concerned, our simulations suggest that, of course, it contributes to reduce the epidemic peak. However, this holds in the case where T is medium–small. At the endemic state, the equilibrium size of the compartment of infectious I^* is a decreasing function of the information coverage and of b.

The delay T is able to destabilize the endemic equilibrium by inducing steady state recurrent epidemics. For $\sigma = 26$, we found that the destabilization is observed for a window of values of T.

Irving et al[14] stressed that the parameter σ, which is the rate of the transfer from the carrier to the infectious state, has major impact in absence of vaccination. We found that σ remains of major relevance also in presence of behavior-dependent vaccinations, with specific effects. It does not only deeply modify the epidemic outbreaks (by reducing the peak of I and increasing that of C), as it is intuitive since it rules how many carriers do become infectious, but it also significantly impact on the onset of recurrent epidemics. Indeed, our numerical analysis suggest that there is a critical value σ_m such that for $\sigma < \sigma_m$ no oscillatory solutions occur, and the size of the above-mentioned "instability window" for T increases with σ. In other words, there is a nonlinear interplay between the epidemics-related parameter σ and the behavior-related parameter T. Finally, note that in the cases where the parameter epsilon can be smaller than one, it does not qualitatively change the behavior of the system.

This study is very preliminary and specific assumptions have been made to make model (5) more tractable. Furthermore, the obtained qualitative results need to be validated by field data, especially as far as the behavioral aspects are concerned. In this regard, the values of the information parameters can be estimated directly from sociological surveys, or indirectly, by means of comparison or fitting with epidemiological data. For instance, in Buonomo and Della Marca,[43] the information coverage, h, and the average information delay, T, were estimated for COVID-19 epidemics during the full lockdown in Italy by using official data regarding hospitalized and deaths (the most reliable data among the ones provided by health agencies and governments). A similar approach could be used for meningitis.

We have considered an ideal vaccine which confer lifelong immunity and 100% protection. This is a simplifying assumption that allows to make the model more tractable and provide the best as possible scenario. Indeed, vaccines

against meningococcal disease are serogroup specific and have varying efficacy and degree of duration of conferred protection. It is known[44] that the meningococcal polysaccharide vaccines have documented high short-term efficacy levels in older children and adults, whereas the efficacy in children under 2 years of age have documented to be low or even nil depending on the serogroup against which they should protect. Furthermore, in schoolchildren and adults, the polysaccharide vaccines appears to provide protection for at least 3 years, but in younger children, the levels of specific antibodies decline rapidly after 2–3 years. However, polysaccharide vaccines are gradually being replaced by polysaccharide-protein conjugate vaccines (like *MenAfriVac*), which confer longer-lasting immunity and are effective in protecting children under 2 years of age.[44] Such vaccines have reduced the burden of meningitis in many countries thereby showing the potential for an "endgame" for meningitis.[45]

Therefore, we plan to study the case of information-dependent *imperfect* vaccine, which could lead to oscillations and hysteresis.[35,46]

Other future investigations will concern (i) the possible interplay between the important seasonal changes of β and also of σ, as stressed in Irving et al,[14] with the behavioral components we introduced here; (ii) the effect of more realistic non-Erlangian kernels (as the *acquisition-fading kernel* introduced in d'Onofrio et al.[47]); (iii) the optimal control of public health strategies aimed at increasing vaccine acceptance.

ACKNOWLEDGEMENTS

The present work has been performed under the auspices of the Italian National Group for the Mathematical Physics (GNFM) of National Institute for Advanced Mathematics (INdAM). The authors B.B., S.M.K., and Y.H.W. gratefully acknowledge the University of Naples Federico II that supported their research through the project entitled *Advanced dynamical systems for the analysis and control of transmission of infectious diseases* in the framework of "NAASCO," bilateral agreement of scientific cooperation between the University of Naples Federico II and the Addis Ababa University. S. M. K. is supported by Botswana International University of Science and Technology (BIUST) through the BIUST Initiation grant DVC/RDI/2/1/161(34). The authors are grateful to the anonymous reviewers for their constructive comments. Open Access Funding provided by Universita degli Studi di Napoli Federico II within the CRUI-CARE Agreement.

CONFLICT OF INTEREST

This work does not have any conflicts of interest.

ORCID

Bruno Buonomo https://orcid.org/0000-0003-4998-3725
Alberto d'Onofrio https://orcid.org/0000-0002-2190-272X
Semu Mitiku Kassa https://orcid.org/0000-0001-5494-040X

REFERENCES

1. Centers for Disease Control and Prevention. Meningitis. https://www.cdc.gov/meningitis/index.html (Accessed on September 2019).
2. World Health Organization. Meningococcal meningitis. https://www.who.int/news-room/fact-sheets/detail/meningococcal-meningitis (Accessed on September 2019).
3. Shmaefsky BR. *Deadly Diseases and Epidemics: Meningitis*. New York: Chelsea House; 2005.
4. Feavers I, Pollard AJ, Sadarangani M (Eds). *Handbook of Meningococcal Disease Management*. Adis; 2016.
5. Trotter CL, Greenwood BM. Meningococcal carriage in the African meningitis belt. *Lancet Infect Dis*. 2007;7(12):797-803.
6. Wireko–Brobby G. Bacterial meningitis and deafness in sub-Saharan Africa. In: Wireko–Brobby G, ed. *Meningitis*. InTech; 2012.
7. Pinner RW, Onyango F, Perkins BA, et al. Epidemic meningococcal disease in Nairobi, Kenya, 1989. *J Infect Dis*. 1992;166(2):359-364.
8. Martcheva M, Crispino-O'Connell G. The transmission of meningococcal infection: a mathematical study. *J Math Anal Appl*. 2003;283:251-275.
9. Tuckwell HC, Hanslik T, Valleron AJ, Flahault A. A mathematical model for evaluating the impact of vaccination schedules: application to Neisseria meningitidis. *Epidemiol Infect*. 2003;130(3):419-429.
10. Trotter CL, Gay NJ, Edmunds WJ. Dynamic models of meningococcal carriage, disease, and the impact of serogroup C conjugate vaccination. *Am J Epidemiol*. 2005;162(1):89-100.
11. Coen PG, Cartwright K, Stuart J. Mathematical modeling of infection and disease due to *Neisseria meningitides* and *Neisseria lactamica*. *Int J Epidemiol*. 2000;29(1):180-188.
12. Simpson JL, Roberts MG. Modelling the effect of vaccination on the meningococcal B epidemic in New Zealand. *The ANZIAM J*. 2012;54(1–2):74-88.

13. Blyuss KB. Mathematical modelling of the dynamics of meningococcal meningitis in Africa. In: Aston PJ, Mulholl AJ, Tant KMM, eds. *UK Success Stories in Industrial Mathematics*. Springer; 2016:221-226.
14. Irving TJ, Blyuss KB, Colijn C, Trotter CL. Modelling meningococcal meningitis in the African meningitis belt. *Epidemiol Infect*. 2012;140(5):897-905.
15. Djatcha Yaleu G, Bowong S, Houpa Danga E, Kurths J. Mathematical analysis of the dynamical transmission of *Neisseria meningitidis* serogroup A. *Int J Comput Math*. 2017;94(12):2409-2434.
16. Manfredi P, d'Onofrio A (Eds). *Modeling the Interplay Between Human Behavior and the Spread of Infectious Diseases*. Springer; 2013.
17. Wang Z, Bauch CT, Bhattacharyya S, et al. Statistical physics of vaccination. *Phys Rep*. 2016;664:1-113.
18. Asfaw MD, Buonomo B, Kassa SM. Impact of human behavior on ITNs control strategies to prevent the spread of vector borne diseases. *Atti Accad Peloritana Pericolanti Cl Sci Fis Mat Natur*. 2018;96(suppl. 3):A2.
19. Colombini A, Bationo F, Zongo S, et al. Costs for households and community perception of meningitis epidemics in Burkina Faso. *Clin Infect Dis*. 2009;49(10):1520-1525.
20. Timmermans DR, Henneman L, Hirasing RA, van der Wal G. Parents' perceived vulnerability and perceived control in preventing meningococcal C infection: a large-scale interview study about vaccination. *BMC Public Health*. 2008;8(1):45.
21. Morrone T, Napolitano F, Albano L, Di Giuseppe G. Meningococcal serogroup B vaccine: knowledge and acceptability among parents in Italy. *Hum Vaccin Immunother*. 2017;13(8):1921-1927.
22. Drozd-Dabrowska M, Topczewska K, Korzen M, Salacka A, Ganczak M. Parental knowledge about meningococcal disease and vaccination uptake among 0–5 years old polish children. *Int J Environ Res Public Health*. 2019;16(2):265.
23. LaForce FM, Djingarey M, Viviani S, Preziosi MP. Successful African introduction of a new Group A meningococcal conjugate vaccine: future challenges and next steps. *Hum Vaccin Immunother*. 2018;14(5):1098-1102.
24. Cooper S, Betsch C, Sambala EZ, Mchiza N, Wiysonge CS. Vaccine hesitancy—a potential threat to the achievements of vaccination programmes in Africa. *Hum Vaccin Immunother*. 2018;14(10):2355-2357.
25. European Centre for Disease Prevention and Control. Catalogue of interventions addressing vaccine hesitancy. https://ecdc.europa.eu/sites/portal/files/documents/Catalogue-interventions-vaccine-hesitancy.pdf (Accessed on September 2019).
26. Anderson RM, May RM. *Infectious Diseases of Humans: Dynamics and Control*. Oxford University Press; 1992.
27. Capasso V. *Mathematical Structures of Epidemic Systems*. Berlin: Springer; 1993.
28. Verelst F, Willem L, Beutels P. Behavioural change models for infectious disease transmission: a systematic review (2010–2015). *J R Soc Interface*. 2016;13(125):20160820.
29. LaForce FM, Ravenscroft N, Djingarey M, Viviani S. Epidemic meningitis due to Group A *Neisseria meningitidis* in the African meningitis belt: a persistent problem with an imminent solution. *Vaccine*. 2009;27:B13-B19.
30. Serra LC, York LJ, Gamil A, Balmer P, Webber C. A review of meningococcal disease and vaccination recommendations for travelers. *Infect Dis Ther*. 2018;7(2):219-234.
31. d'Onofrio A, Manfredi P, Salinelli E. Bifurcation thresholds in an SIR model with information-dependent vaccination. *Math Model Nat Phenom*. 2007;2(1):26-43.
32. d'Onofrio A, Manfredi P, Salinelli E. Vaccinating behaviour, information, and the dynamics of SIR vaccine preventable diseases. *Theor Popul Biol*. 2007;71(3):301-317.
33. Buonomo B, d'Onofrio A, Lacitignola D. Global stability of an SIR epidemic model with information dependent vaccination. *Math Biosci*. 2008;216(1):9-16.
34. Buonomo B, d'Onofrio A, Lacitignola D. The geometric approach to global stability in Behavioral Epidemiology. In: Manfredi P, d'Onofrio A, eds. *Modeling the Interplay Between Human Behavior and the Spread of Infectious Diseases*. Springer; 2013:289-308.
35. Buonomo B, Della Marca R. Oscillations and hysteresis in an epidemic model with information-dependent imperfect vaccination. *Math Comput Simulation*. 2019;162:97-114.
36. Kumar A, Srivastava PK, Gupta RP. Nonlinear dynamics of infectious diseases via information-induced vaccination and saturated treatment. *Math Comput Simulation*. 2019;157:77-99.
37. MacDonald N. *Biological Delay Systems: Linear Stability Theory*. Cambridge University Press; 1989.
38. van den Driessche P, Watmough J. Reproduction numbers and sub-threshold endemic equilibrium for compartmental models of disease transmission. *Math Biosci*. 2002;180(1-2):29-48.
39. Kamgang JC, Sallet G. Computation of threshold conditions for epidemiological models and global stability of the disease-free equilibrium (DFE). *Math Biosci*. 2008;213(1):1-12.
40. Kolaye GG, Bowong S, Houe R, Aziz-Alaoui MA, Cadivel M. Mathematical assessment of the role of environmental factors on the dynamical transmission of cholera. *Commun Nonlinear Sci Numer Simul*. 2019;67:203-222.
41. Castillo-Chavez C, Song B. Dynamical models of tuberculosis and their applications. *Math Biosci Eng*. 2004;1:361-404.
42. Dushoff J, Huang W, Castillo-Chavez C. Backward bifurcations and catastrophe in simple models of fatal diseases. *J Math Biol*. 1998;36(3):227-248.
43. Buonomo B, Della Marca R. Effects of information-induced behavioural changes during the COVID–19 lockdowns: the case of Italy. *R Soc Open Sci*. 2020;7(10):201635.
44. World Health Organization. Meningococcal disease. https://www.who.int/ith/vaccines/meningococcal/en/ (Accessed on April 2021).
45. Maiden MC. The impact of protein-conjugate polysaccharide vaccines: an endgame for meningitis? *Philos Trans R Soc Lond B Biol Sci*. 1623;2013(368):20120147.

46. d'Onofrio A, Manfredi P. Bistable endemic states in a susceptible–infectious–susceptible model with behavior-dependent vaccination. In: Chowell G, Hyman JM, eds. *Mathematical and Statistical Modeling for Emerging and Re-emerging Infectious Diseases*. Springer; 2016:341-354.
47. d'Onofrio A, Manfredi P, Salinelli E. Vaccinating behaviour and the dynamics of vaccine preventable infections. In: Manfredi P, d'Onofrio A, eds. *Modeling the Interplay Between Human behavior and the Spread of Infectious Diseases*. Springer, New York; 2013:267-287.

How to cite this article: Buonomo B, d'Onofrio A, Kassa SM, Workineh YH. Modeling the effects of information-dependent vaccination behavior on meningitis transmission. *Math Meth Appl Sci*. 2022;45: 732-748. https://doi.org/10.1002/mma.7808